

## Differential phase shift in nonreciprocal microstrip lines on magnetic nanowired substrates

J. De La Torre Medina, J. Spiegel, M. Darques, L. Piraux, and I. Huynen

Citation: *Appl. Phys. Lett.* **96**, 072508 (2010); doi: 10.1063/1.3313942

View online: <http://dx.doi.org/10.1063/1.3313942>

View Table of Contents: <http://apl.aip.org/resource/1/APPLAB/v96/i7>

Published by the [American Institute of Physics](#).

---

### Additional information on *Appl. Phys. Lett.*

Journal Homepage: <http://apl.aip.org/>

Journal Information: [http://apl.aip.org/about/about\\_the\\_journal](http://apl.aip.org/about/about_the_journal)

Top downloads: [http://apl.aip.org/features/most\\_downloaded](http://apl.aip.org/features/most_downloaded)

Information for Authors: <http://apl.aip.org/authors>

## ADVERTISEMENT



**HAVE YOU HEARD?**

Employers hiring scientists  
and engineers trust  
**physicstoday JOBS**



<http://careers.physicstoday.org/post.cfm>

# Differential phase shift in nonreciprocal microstrip lines on magnetic nanowired substrates

J. De La Torre Medina,<sup>1,a)</sup> J. Spiegel,<sup>2</sup> M. Darques,<sup>1</sup> L. Piraux,<sup>1</sup> and I. Huynen<sup>2,a)</sup>

<sup>1</sup>Unité de Physico-Chimie et de Physique des Matériaux, Université Catholique de Louvain, Place Croix du Sud 1, B-1348 Louvain-la-Neuve, Belgium

<sup>2</sup>Laboratoire d'Hyperfréquences (EMIC), Université Catholique de Louvain, Place du Levant 3, B-1348 Louvain-la-Neuve, Belgium

(Received 28 September 2009; accepted 19 January 2010; published online 17 February 2010)

Nonreciprocal microstrip lines based on magnetic nanowired substrates were fabricated for the characterization of microwave differential phase shifts. We provide a fully integrated solution for the nonreciprocal edge guided mode, which is achieved by asymmetrically loading the width of the microstrip with nanowires of different heights. An analytical model explaining the microwave nonreciprocal propagation, which takes into account the substrate permittivity and the microstrip memductance, is validated with the experiment. © 2010 American Institute of Physics.

[doi:10.1063/1.3313942]

Arrays of magnetic nanowires (NWs) embedded into porous templates, also known as magnetic nanowired substrates (MNWS), are nowadays interesting for the fabrication of microstrip microwave devices. Previous works on these devices include circulators,<sup>1</sup> magnetic photonic band gap materials,<sup>2</sup> isolators,<sup>3</sup> and noise suppressors.<sup>4</sup> We have previously demonstrated the feasibility of self-biased circulators using MNWS,<sup>1</sup> which exhibit nonreciprocal behavior at the microwave range. Besides, nonreciprocal propagation in transmission lines involving ferromagnetic or ferrite materials is usually obtained via the Faraday rotation effect, which requires a magnetic field pattern with elliptical or circular polarization. This polarization is usually observed in metallic rectangular waveguides or in coplanar waveguide topologies.<sup>3,5</sup> Another solution, proposed by Hines,<sup>6</sup> is particularly suited to microstrip topologies. In such lines, the presence of a ferromagnetic material under the microstrip induces a nonuniformity of the microwave energy, specifically a displacement of the electric field pattern along the width of the strip, such that it concentrates preferably near one long edge of the microstrip. This electric field pattern is reversed with respect to the symmetry axis of the microstrip when either the propagation sense or the direction of an external dc biasing magnetic field is reversed. If the microstrip is not symmetrically loaded at its two long edges, for example, by inserting substrates having different dielectric constants, the propagation along the line becomes nonreciprocal, because, depending on the propagation sense, the field concentration moves from one dielectric medium to the other. The so-called edge-guided mode nonreciprocal devices have two following main applications: isolators<sup>7,8</sup> and nonreciprocal phase shifters<sup>9</sup> for gyrators<sup>10</sup> and electronically phased arrays antennas.<sup>11</sup> The nonreciprocal operation, which is induced by asymmetrically loading the two long edges of the microstrip, requires an usually difficult cointegration over the width of the strip of substrates having different permittivities or losses. In this paper, we propose a fully integrated solution for the edge-guided mode

in nonreciprocal microstrip lines (NRML) on MNWS, which is suited for differential phase shift performances at room temperature. This device does not require the assembly of different substrates, since the variation in the permittivity along the width of the strip is simply induced by an asymmetric filling of the substrates with NWs. We have indeed recently demonstrated that the effective permittivity of a MNWS under a microstrip is strongly dependent on the NWs height.<sup>12</sup>

The fabrication of NRML on MNWS is done by electrodeposition of Ni NWs into the pores of polycarbonate (PC) membranes<sup>13</sup> with thickness  $h_p=21\ \mu\text{m}$ , as reported elsewhere.<sup>14</sup> The membrane porosity  $P$  is 12% while the NWs diameter  $d$  is 50 nm. The asymmetric filling of the substrate is carried out in several steps in order to obtain three adjacent strip zones with widths  $w_1=100\ \mu\text{m}$ ,  $w_2=150\ \mu\text{m}$ , and  $w_3=250\ \mu\text{m}$ , as shown schematically in Fig. 1(a). Step 1 consists in evaporating a 300 nm thick, 3 mm wide, and 3 cm long cathode for electrodeposition on one side of the membrane. Part of the membrane cathode is in contact with an exposed part of a platinum plate to make electrical contact. The rest of the plate is covered with isolating tape to avoid electrodeposition on it. The side of the

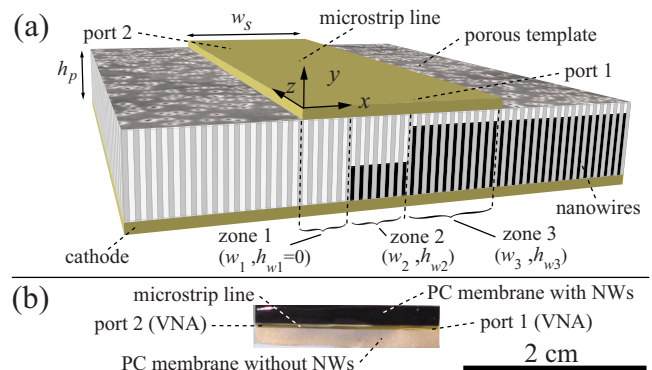


FIG. 1. (Color online) (a) Schematics of the NRML on a MNWS. The microstrip line cross section is divided in three slab zones with widths  $w_1=100\ \mu\text{m}$ ,  $w_2=150\ \mu\text{m}$ , and  $w_3=250\ \mu\text{m}$  and wire heights  $h_{w1}=0$ ,  $h_{w2}\approx 0.3h_p$  and  $h_{w3}\approx 0.88h_p$ , respectively. (b) Photograph for the NRML on a MNWS for which the microstrip line is asymmetrically loaded with NWs as shown in (a).

<sup>a)</sup> Authors to whom correspondence should be addressed. Electronic addresses: joaquin.delatorre@uclouvain.be and isabelle.huynen@uclouvain.be.

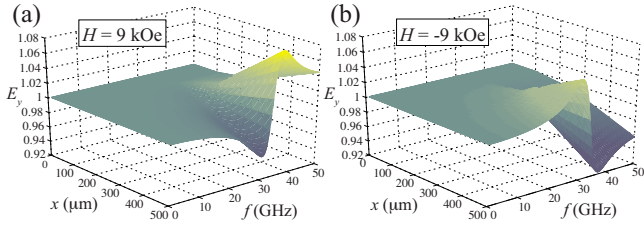


FIG. 2. (Color online) Three-dimensional view of the electric field pattern  $E_y$  as a function of the position  $x$  along the cross section of the microstrip line and the excitation frequency  $f$  under the application of a magnetic field  $H$  of (a) 9 kOe and (b)  $-9$  kOe.

PC membrane exposed to the electrolyte is masked to select a length of 2 cm over the evaporated cathode. Then the NWs growth is done until their height is  $h_{w_3} - h_{w_2}$ . In steps 3 and 4, a second cathode layer over the PC membrane besides the first cathode is evaporated, and the wires are grown over the surface of step 2 and over a  $150 \mu\text{m}$  wide and 2 cm long strip over the second cathode, respectively. Growth of the NWs is then performed until the NWs height  $h_{w_2}$  is  $0.3h_p$  over the second cathode layer [zone 2 in Fig. 1(a)] and  $h_{w_3}$  is  $0.88h_p$  over the first one [zone 3 in Fig. 1(a)]. Finally, in step 5 a microstrip line of width  $w_s = 500 \mu\text{m}$  and length  $L = 2$  cm is evaporated over the side of the membrane opposite to the cathode as shown by the photograph of Fig. 1(b), so defining three slab zones with different NWs heights [see Fig. 1(a)].

On the other hand, the operation of the NRML as an edge-guided mode device is predicted assuming a nonuniform  $y$ -component ( $E_y$ ) of the electric field pattern across the  $x$  position of the transverse section of the microstrip line, using a formalism adapted from the one proposed by Hines<sup>6</sup>

$$E_{y_1} = 1 + A \quad \text{for } 0 \leq x \leq w_1, \quad (1)$$

$$E_{y_2} = A + e^{-\alpha_2(x-w_1)} \quad \text{for } w_1 \leq x \leq w'_2, \quad (2)$$

$$E_{y_3} = (A + e^{-\alpha_2 w_2})e^{-\alpha_3(x-w'_2)} \quad \text{for } w'_2 \leq x \leq w_s, \quad (3)$$

where  $w'_2 = w_1 + w_2$  and  $w_s = w_1 + w_2 + w_3$ . In these equations,  $\alpha_i = j\kappa_i k_z / \mu_i$  are attenuation factors for  $i=1, 2, 3$  with  $k_z$  the propagation constant along the  $z$ -axis of the microstrip,  $j\kappa_i$  and  $\mu_i$  are, respectively, the off-diagonal and diagonal terms of the permeability tensor  $\bar{\mu}$  in each zone, which are given by

$$\mu_i = 1 + 2\pi M_s \gamma P h_w f_r (f_r^2 - f^2)^{-1} (m^2 + 1), \quad (4)$$

$$\kappa_i = 4\pi M_s \gamma P h_w f (f_r^2 - f^2)^{-1} m. \quad (5)$$

In these equations  $f_r = \gamma[H + 2\pi M_s(1 - 3P)] + j\alpha f$  is the resonance frequency,  $m = M/M_s$  is the normalized magnetization,  $\alpha$  is the damping factor,  $H$  is the static field applied parallel to the NWs,  $f$  is the rf-frequency, and  $M_s = 485 \text{ emu cm}^{-3}$  and  $\gamma = 3.09 \text{ GHz kOe}^{-1}$  are the saturation magnetization and the gyromagnetic ratio for Ni, respectively.<sup>1</sup>

The magnitude of  $E_y$  as a function of  $x$  and  $f$  is shown in Fig. 2 for a saturating field  $H$  of (a) 9 kOe and (b)  $-9$  kOe. As seen,  $E_y$  is asymmetrical along the transverse  $x$ -axis at frequencies in the vicinity of  $f_r = 34$  GHz. The first zone ( $0 < x < w_1$ ) is not filled with NWs ( $h_{w_1} = 0$ ), implying an isotropic permeability,  $\mu_1 = 1$  and  $\kappa_1 = 0$  [see Eqs. (4) and

(5)]. Therefore  $\alpha_1 = 0$  and  $E_y$  is constant [see Eq. (1)]. As seen from Fig. 2(a),  $E_y$  decreases in zone 3 for  $f < f_r$  with minimum at  $f \approx 31$  GHz, indicating a displacement of microwave energy toward zone 1. As  $f$  is further increased such that  $f > f_r$ ,  $\kappa_i$  changes its sign from positive to negative, inducing a field displacement toward zone 3 with maximum  $E_y$  magnitude at  $f \approx 36$  GHz. Besides, the  $E_y$  displacement is inverted as  $H$  is inverted ( $m = -1$ ), as seen from Fig. 2(b), implying a change of sign in  $\kappa_i$  and  $\alpha_i$  for zones 2 and 3 along the  $x$ -axis which can also be achieved by changing the sign of  $k_z$ , other said the propagation sense. In this case  $E_y$  is now concentrated in zone 3 for  $f < f_r$  and in zone 1 for  $f > f_r$ . The nonreciprocal behavior is achieved by combining this edge-guided mode behavior with a change of permittivity from zone 1 to zone 3, such that  $\epsilon_1 = 2.66$ ,  $\epsilon_2 = 3.8$ , and  $\epsilon_3 = 22.2$ , which is induced by the change in NWs height.<sup>12</sup> Based on this electric field modeling, the propagation of electromagnetic waves can be successfully predicted using the theory of nonreciprocal transmission lines including the memductance concept introduced by Marqués *et al.*<sup>15</sup> The addition of the memductance  $M$  in the classical  $LC$  equivalent circuit of the microstrip line section enables to calculate the nonreciprocal complex propagation constants  $k_{\pm}$  in the forward (+) and backward (−)  $z$ -direction as

$$k_{\pm} = \frac{jk_z^2}{2\pi f} [-M/C \pm \sqrt{(M/C)^2 - (2\pi f/k_z)^2}]. \quad (6)$$

In this equation,  $k_z$  is the complex propagation constant of the reciprocal line with uniform NWs height  $h_w = \sum_{i=1}^3 h_{w_i}/3$  over its cross section, which is obtained from a variational approach.<sup>16</sup> Next,  $C = \epsilon_0 \sum_{i=1}^3 \epsilon_{r_i} w_i / h_p$  is the microstrip capacitance of the NRML and  $M$  is the memductance obtained according to the formulation of Marques *et al.*<sup>17</sup> as

$$M = \frac{j2\pi f \epsilon_0}{k_z h_p} \sum_{i=1}^3 \int_{I_i} \epsilon_{r_i} E_{y_i}(x) dx, \quad (7)$$

where  $I_i$  are the intervals in the  $x$ -axis for each  $E_{y_i}$ . Imposing  $M = 0$  when the microstrip is symmetrically loaded ( $\epsilon_{r_1} = \epsilon_{r_2} = \epsilon_{r_3}$ , implying reciprocal behavior), fixes constant  $A$  in expressions (1)–(3).

The key parameter for predicting the isolation  $\Delta S = S_+ - S_-$  and differential phase shift  $\Delta\varphi = \varphi_+ - \varphi_-$  of the NRML of length  $L$  is the constant  $k_{\pm}$ , which is related to the transmission  $T_{\pm} = e^{-k_{\pm} L}$  in the (+) and (−) directions. This yields the insertion losses  $S_{\pm} = -20 \log_{10} |T_{\pm}| = 20L \Re(k_{\pm}) \log_{10} e$  and phase shifts  $\varphi_{\pm} = L \Im(k_{\pm})$ , from which  $\Delta S/L$  and  $\Delta\varphi/L$  are obtained. Measurements of  $\Delta S/L$  and  $\Delta\varphi/L$  at fixed field values have been performed using a vector network analyzer (VNA) after saturating the device to 10 kOe. The (+) and (−) propagation directions refer to propagations from ports 1 to 2 and from 2 to 1 of the VNA, respectively. Figure 3(a) shows measured (symbols) and calculated (continuous lines)  $\Delta\varphi/L$  for positive and negative  $H$  values (numbers, in kilooersted) for the NRML (gray and black symbols) and for a symmetrically loaded microstrip line (squares with crosses), and a good agreement is found. Comparing Figs. 2(a) and 2(b) and Fig. 3(a) for the NRML, we see that a concentration of  $E_y$  in zones 1 and 3 leads to negative and positive  $\Delta\varphi/L$ , respectively. For instance, for  $H = 9$  kOe  $\Delta\varphi/L$  is negative for  $f < f_r$  and positive for  $f > f_r$ , as  $E_y$  is concentrated in zones 1 and 3 for  $f < f_r$  and  $f > f_r$ , respectively. The ampli-

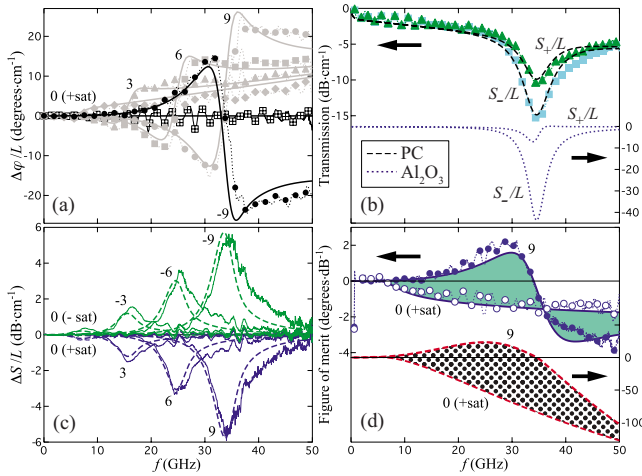


FIG. 3. (Color online) (a) Calculated (continuous lines) and measured  $\Delta\varphi/L$  for a symmetrically loaded microstrip line (squares with crosses) and for the NRML of Fig. 1(b), for positive (gray symbols) and negative (black symbols) field values. (b) Measured (symbols) and calculated (dashed lines)  $S_{\pm}/L$  at 9 kOe for the NRML of (a) and calculated ones (dotted lines) for a NRML on a 60  $\mu\text{m}$  thick  $\text{Al}_2\text{O}_3$  substrate. (c) Measured (continuous lines) and calculated (dotted lines)  $\Delta S/L$  for the NRML of (a). (d) Measured (symbols) and calculated (filled region) FOM in the range 0–9 kOe for the NRML of (a) and for the NRML on  $\text{Al}_2\text{O}_3$  considered in (b) (patterned region). In all figures, the field values denoted as numbers are given in kilo-ersted.

tude of  $\Delta\varphi/L$  decreases by decreasing  $H$  and remains almost constant for  $f > f_r$ . Inverting the magnetic field direction leads to an inversion of  $\Delta\varphi/L$ , as in the case of  $E_y$ , evidencing the nonreciprocity of the device [black symbols for  $H = -9$  kOe in Fig. 3(a)]. Interestingly,  $\Delta\varphi/L$  is nonzero at zero field, due to the single domain feature of the NWs at remanence, and can be tuned in the range  $\pm 10^\circ \text{cm}^{-1}$ . This is,  $\Delta\varphi$  depends on the NWs magnetic state  $m$  by virtue of Eq. (5). Besides,  $\Delta\varphi/L$  is negligible for the symmetrically loaded microstrip line, corroborating the fact that an asymmetric dielectric loading of the microstrip cross section is necessary for observing a nonzero  $\Delta\varphi$ . Both measured (symbols) and calculated (dashed lines)  $S_{\pm}/L$  at 9 kOe and  $\Delta S/L$  are shown in Figs. 3(b) and 3(c), respectively, and show good agreement. Inverting  $H$  leads to an inversion of absorption depths for each propagation direction and a change of sign in  $\Delta S/L$ , due to the nonreciprocal feature of the device. However, the performances as isolator are poor because the maximal isolation occurs at  $f = f_r$ , where insertion losses are maximal. On the contrary, optimal  $\Delta\varphi/L > 20^\circ \text{cm}^{-1}$  is obtained when  $f > f_r$ , where FMR losses and  $\Delta S/L$  tend to zero [see Figs. 3(b) and 3(c)]; residual losses on  $S_{\pm}/L$  correspond to dielectric losses of the substrate. They are reduced by using porous templates with loss tangent factor  $\tan \delta \leq 0.05$  (value for PC). For instance, Fig. 3(b) shows calculated  $S_{\pm}/L$  (dotted lines) for a NRML on a 60  $\mu\text{m}$  thick  $\text{Al}_2\text{O}_3$  template for which  $\tan \delta \approx 0.001$ . Same parameters  $h_{w_i}/h_p$  ( $i = 1, 2, 3$ ),  $w_1$  and  $w_3$  as for the NRML of Fig. 1 are used, while  $w_2 = 380 \mu\text{m}$ . Since the relative permittivity of  $\text{Al}_2\text{O}_3$  (9.8) is higher than the one of PC (2.89), a stronger field displacement is expected, and higher  $\Delta S/L = 42 \text{ dB cm}^{-1}$  and  $\Delta\varphi/L = 81^\circ \text{cm}^{-1}$  performances are predicted for  $H = 9$  kOe (not shown). Besides, Fig. 3(d) shows measured (symbols) and calculated (continuous lines) figure of merit FOM

$= 2\Delta\varphi/(S_+ + S_-)$ , which varies within the filled region delimited by FOM for 0 and 9 kOe and is of about  $2-3^\circ \text{dB}^{-1}$  for  $f > f_r$ . These values are lower than reported ones for devices based on ferrites, in the range  $38-130^\circ \text{dB}^{-1}$  at x-band and 300 K.<sup>5,18</sup> However, the calculated FOM for the NRML on  $\text{Al}_2\text{O}_3$  of Fig. 3(b) is in the range  $100-130^\circ \text{dB}^{-1}$  at 50 GHz, with highest value at zero field, as shown in Fig. 3(d) (patterned region). This is of potential interest for the realization of a gyrator element ( $\Delta\varphi = 180^\circ$ ) operating at 50 GHz and 300 K with low insertion losses: it can be obtained with a 2.2 cm long NRML on  $\text{Al}_2\text{O}_3$  templates. This advantageously compares with conventional devices based on ferrites that exhibit  $\Delta\varphi/L$  between  $20-53^\circ \text{cm}^{-1}$  in a frequency range limited to 10 GHz.<sup>5,11,19,20</sup>

In conclusion, we have fabricated a planar fully integrated NRML on a MNWS, which is based on a field displacement mechanism and is of potential use as planar microwave nonreciprocal phase shifter operating around 50 GHz. The model including the MNWS permittivity and the microstrip memductance shows an excellent agreement with experiment.

This work was partly supported by the Interuniversity Attraction Poles Program (P6/42)-Belgian State-Belgian Science Policy. M.D. and I.H. are respectively Fellow and Research Director of Research Science Foundation (FRS-FNRS), Belgium. The authors would like to thank P. Simon for his help and advice.

- <sup>1</sup>A. Saib, M. Darques, L. Piroux, D. Vanhoenacker-Janvier, and I. Huynen, *J. Phys. D* **38**, 2759 (2005).
- <sup>2</sup>A. Saib, D. Vanhoenacker-Janvier, I. Huynen, A. Encinas, L. Piroux, E. Ferain, and R. Legras, *Appl. Phys. Lett.* **83**, 2378 (2003).
- <sup>3</sup>B. K. Kuanr, V. Veerakumar, R. Marson, S. R. Mishra, R. E. Camley, and Z. J. Celinski, *Appl. Phys. Lett.* **94**, 202505 (2009).
- <sup>4</sup>B. K. Kuanr, R. Marson, S. R. Mishra, A. V. Kuanr, R. E. Camley, and Z. J. Celinski, *J. Appl. Phys.* **105**, 07A520 (2009).
- <sup>5</sup>C. P. Wen, *IEEE Trans. Microwave Theory Tech.* **17**, 1087 (1969).
- <sup>6</sup>M. E. Hines, *IEEE Trans. Microwave Theory Tech.* **19**, 442 (1971).
- <sup>7</sup>E. Schloemann, *J. Magn. Magn. Mater.* **209**, 15 (2000).
- <sup>8</sup>S. H. Talisa and D. M. Bolle, *IEEE Trans. Microwave Theory Tech.* **27**, 584 (1979).
- <sup>9</sup>D. M. Bolle and S. H. Talisa, *IEEE Trans. Microwave Theory Tech.* **27**, 878 (1979).
- <sup>10</sup>J. Mazur, M. Mazur, J. Michalski, and E. Sedek, Proceedings of the 14th International Conference on Microwave, Radar, and Wireless Communication, 2002, Vol. 1, p. 245.
- <sup>11</sup>J. Mielewski and A. Buda, Proceedings of the 12th International Conference on Microwave and Radar, MIKON, 1998, Vol. 2, p. 509.
- <sup>12</sup>J. Spiegel, J. De La Torre, M. Darques, L. Piroux, and I. Huynen, *IEEE Microw. Wirel. Compon. Lett.* **17**, 492 (2007).
- <sup>13</sup>E. Ferain and R. Legras, *Nucl. Instrum. Methods Phys. Res. B* **208**, 115 (2003).
- <sup>14</sup>J. De La Torre Medina, M. Darques, and L. Piroux, *J. Phys. D: Appl. Phys.* **41**, 032008 (2008).
- <sup>15</sup>R. Marqués, F. Mesa, and F. Medina, *IEEE Microw. Guid. Wave Lett.* **10**, 225 (2000); *IEEE Microw. Wirel. Compon. Lett.* **11**, 467 (2001).
- <sup>16</sup>J. Spiegel and I. Huynen, *J. Comput. Theor. Nanosci.* **6**, 2001 (2009).
- <sup>17</sup>R. Marqués, F. Mesa, and F. Medina, *Microwave Opt. Technol. Lett.* **38**, 3 (2003).
- <sup>18</sup>G. F. Dionne, D. E. Oates, D. H. Temme, and J. A. Weiss, *IEEE Trans. Microwave Theory Tech.* **44**, 1361 (1996).
- <sup>19</sup>J. Zafar, A. A. P. Gibson, and H. R. Zafar, Proceedings of the Third European Conference on Antennas and Propagation, EUCAP, 2009, p. 3029.
- <sup>20</sup>W. Junding, Y.-Z. Xiong, M.-J. Shi, G.-F. Chen, and M.-D. Yu, *IEEE Trans. Microwave Theory Tech.* **42**, 616 (1994).